THE EFFECT OF HIGH-*K* PASSIVATION LAYER ON OFF-STATE BREAKDOWN VOLTAGE OF AlGaAs/InGaAs HEMT

S. X. SUN[a,d], Y. H. ZHONG[b*], H. Y. MEI[a], R. X. YAO[a], F. J. CHEN[a],
Y. X. LI[b], Y. F. HU[c]

[a]*Henan Provincial Key Laboratory of Smart Lighting,School of Information Engineering, Huanghuai University, Zhumadian 463000, China*
[b]*School of Physics and Microelectronics , Zhengzhou University, Zhengzhou 450001, China*
[c]*Microelectronics Institute, Xidian University, Xi'an 710071, China*
[d]*Henan International Joint Laboratory of Behavior Optimization Control for Smart Robots, Zhumadian 463000, China*

In this paper, the effects of different relative permittivity (ε_r) of the passivation layer on off-state breakdown voltage of AlGaAs/InGaAs HEMTs are analyzed by ISE-TCAD. It is shown that as ε_r value increases, the off-state breakdown voltage increases. When the ε_r value increased to 80, the off-state breakdown voltage increased from 17.23V to 24.13V by 40.9%. This is because the peak value of electric field at the proximity of gate edge is reduced with the increase of ε_r value and it can lead to the improvement of the off-state breakdown voltage of device. Meanwhile, the electric field peak value near the drain edge increases with the increase of the ε_r value, leading to an increase in the ionization probability of electron-hole ionization under the the grid-drain area. In addition, the results also show that the channel current (I_{DS}) and transconductance (g_m) of the device are slightly reduced by the passivation layer with a high ε_r value, while the specific channel on-resistance is hardly degraded. Therefore, the passivation layer with a high ε_r value can effectively improve the breakdown voltage of the device without sacrificing the DC characteristics of the device.

1. Introduction

With the rapid development of the semiconductor industry, microelectronic devices have made great progress in speed and performance and have become a basic part of high frequency communication systems, such as 5G communication system[1,2]. Due to ultra-fast carrier relaxation time, high breakdown field and high electron mobility, III-V compound semiconductor

---

* Corresponding author: zhongyinghui@zzu.edu.cn

materials are widely used in a variety of high-frequency and high-power microelectronic devices [3,4].

Gallium arsenide (GaAs) is a III-V compound semiconductor material with high saturated electron velocity and high electron mobility, and its electrical properties are far superior to silicon materials, which has widely used in high-frequency devices[5]. GaAs based HEMTs are emerging as the most promising candidates for RF components due to their excellent high frequency, high power and low noise performance [6], such as low noise or power amplifiers for the next generation of commercial wireless communication systems [7]. With the development of new epitaxial technology and nano-gate photolithography, the maximum oscillation frequency (f_{max}) of 20 nm GaAs based HEMT device has reached 1270 GHz[8]. In addition, the largest available GaAs wafer can be up to 6 inches, which could reduce the device manufacturing costs and further promote the widespread use of GaAs based HEMT devices[5]. However, when devices are applied to various products, reliability becomes one of the most pronounced problems that must be solved. The breakdown voltage is not only one of the important factors affecting reliability, but also the application of devices in high power.

In recent years, the method of improving the electric field near the gate edge by introducing the field plate structure has been widely used to improve the breakdown voltage of HEMT devices[9-13]. However, the introduction of the field plate structure will increase the parasitic capacitance of the HEMT device and adversely affect the frequency performance of the device[14]. Therefore, it is necessary to improve the breakdown voltage of the device without affecting other characteristics of the device[5]. Ghander et al. reported that the introduction of SiO_2 passivating layer could effectively improve the breakdown voltage of AlGaN/GaN HEMT device, while the grate-source and grate-leakage capacity of the device were not increased [15]. Zhong et al reported that the introduction of Si_3N_4 passivating layer at 50 nm simultaneously improved the breakdown voltage and DC characteristics of InP based HEMT devices [16]. Lin et al. used 80 nm SiN_X passivating layer to increase the breakdown voltage of AlGaAs/InGaAs HEMT devices and at the same time improve the frequency characteristics of the devices, increasing the f_{max} of the devices by 67.5%[17]. Therefore, the passivation layer is an effective method to improve the breakdown characteristics of the device while balancing the other characteristics of the device. However, most of the passivation materials reported are concentrated in materials with a relatively low dielectric constant (ε_r). In addition, the effect of passivating materials with high ε_r value on the breakdown characteristics of AlGaAs/InGaAs HEMT devices has been rarely reported experimentally and theoretically. Therefore, the effect high-k passivation layer on the breakdown characteristics of AlGaAs/InGaAs HEMT devices was investigated using a two-dimensional simulation method, and the effect of a passivation layer with a high ε_r value on the DC characteristics of the device was discussed. The results show that when the passivation layer ε_r value is 80 (TiO_2), the breakdown voltage of the device is increased by 40.9%, and the DC characteristic of the device is only slightly degraded. Therefore, the high-k passivation layer is an effective method to improve the breakdown voltage of the device and and balance the DC characteristics of the device.

2. Device structure and simulation model

Figure 1 shows the schematic cross section of AlGaAs/InGaAs HEMT. The device structure includes passivation layer, GaAs cap layer, AlGaAs barrier layer, AlGaAs isolation layer, InGaAs channel layer and GaAs substrate. The parameters of the device structure are given in Table 1.A good source-drain ohmic contact was achieved by the heavily doped GaAs cap layer. The source-drain spacing of 1.5 um, and the gate length of the device is 0.25 um.The ε_r of passivation layer materials are varied between 1 and 80 [18, 19].
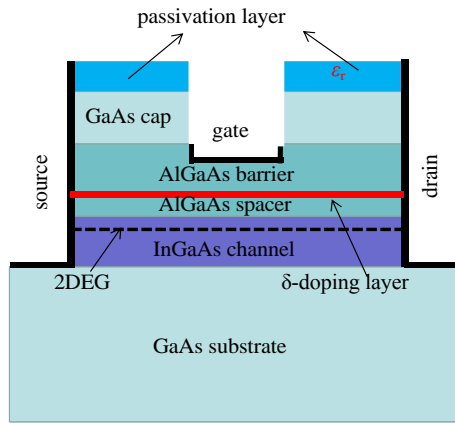
Fig. 1. Schematic cross-section diagram of the AlGaAs/InGaAs HEMT.

Table 1. AlGaAs/InGaAs HEMT device dimension.

Layer	Thickness
Passivation layer	100 nm
GaAs cap layer	30 nm
$Al_{0.3}Ga_{0.7}As$ barrier layer	31 nm
$Al_{0.3}Ga_{0.7}As$ spacer layer	3.5 nm
$In_{0.75}Ga_{0.25}As$ channel layer	10 nm
GaAs substrate	800 nm

In this paper, the Hydrodynamic transport model (HD) was introduced to depict the charge transport properties. The Poisson equation, continuity equation and energy conservation equation were solved[20, 21]. In order to obtain accurate device breakdown characteristics under strong electric field, impact ionization model is introduced in the simulation[22-24]. The generation rate in the impact ionization model can be expressed as

$$G = \frac{\left(\alpha_n |J_n| + \alpha_p |J_p|\right)}{q}$$

where α_n is the ionization rate of electron, α_p is the ionization rate of electron, written as:

$$\alpha_n = A_n \exp\left(\frac{-B_n}{|E|}\right)$$

$$\alpha_p = A_p \exp\left(\frac{-B_p}{|E|}\right)$$

where E is the electric field，and A_n，B_n，A_p and B_p are the fitting parameter[25].Besides, several crucial physical models were also taken into account in the simulation. For describing the doping-dependent and high-field-dependent mobility, the Arora doping-dependent mobility model and Canli high field saturation mobility model were adopted[8, 21]. For considering the recombination process, the Schockley-Read-Hall carrier recombination model was adopted[26].

3. Results and discussion

The breakdown characteristics of AlGaAs/InGaAs HEMT with different passivation layer are shown in Fig.2. The breakdown voltage is defined as the drain voltage when the drain leakage current reaches 1 mA /mm. With the ε_r value increasing from 1 to 80, the breakdown voltage gradually increases and the leakage current gradually decreases.This is mainly because the higher ε_r value of the passivation layer, the much reduced peak value of the electric field at the gate edge and the increased breakdown voltage of the device. In addition, it is also found in Fig.2 (b) that when the ε_r value is relatively small, I_{DS} suddenly increases and the device breaks down. This is because when the ε_r value is low, under reverse bias, the Schottky impact ionization generates a new electron-hole pair, resulting in a sudden increase in gate current (I_{GS}), and leading to a direct gate breakdown[26], as shown in Figure 3.With the increase of the ε_r value, I_{GS} value decreased. Therefore, the phenomenon of arbitrary increase was disappeared.
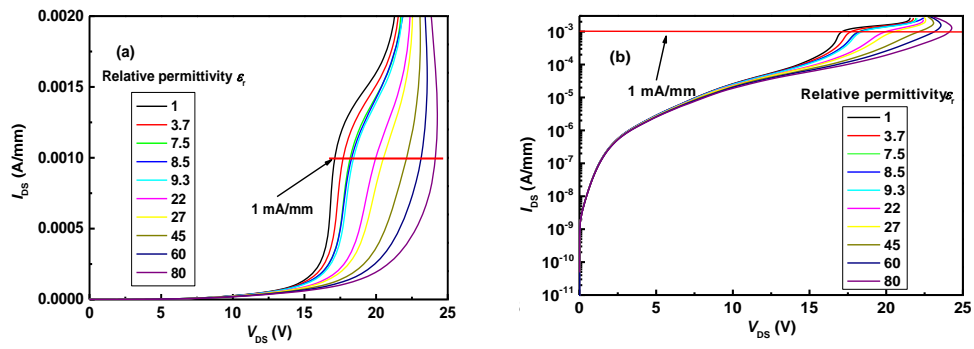
Fig. 2. The normally-off I_{DS}-V_{DS} curves of the AlGaAs/InGaAs HEMT with different passivation layers.
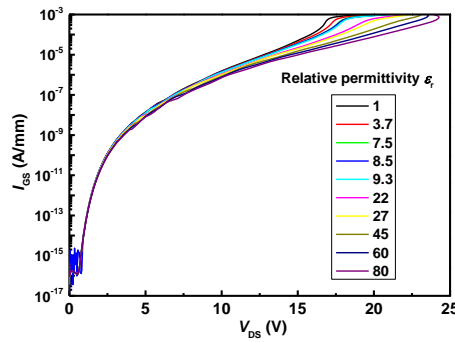
Fig. 3. I_{GS}-V_{DS} curves of the device with different passivation layers.

Figure 4 shows the variation of the breakdown voltage with the εr value. As the εr value varies from 1 to 80, the breakdown voltage increases from 17.12 V to 24.13 V by 40.9%. Due to the peak electric field at the gate electrode edge causing the electron-hole pair ionization, the device leakage current will rapidly increase to avalanche condition. After the passivation layer is introduced, the peak value of the electric field near the gate electrode edge is effectively reduced, and the leakage current formed by the drain current emitted from the gate is reduced, thus increasing the breakdown voltage of the device. With the increase of ε_r, the peak value of the electric field near the gate decreases more obviously, and the voltage required to achieve the device breakdown is also higher. Therefore, the greater the dielectric value of ε_r, the higher the device breakdown voltage.
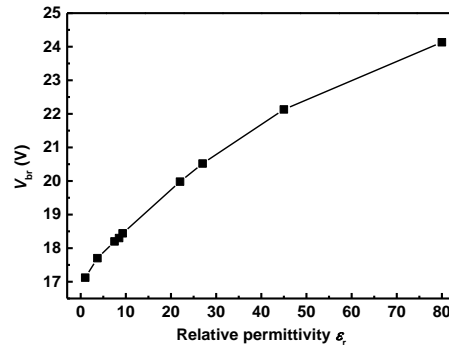
Fig. 4. Off-state breakdown voltage versus εr value of the passivation layer.

Fig. 5 shows the distribution of the electric field at the breakdown of the device with different ε_r values. It can be seen that the passivation layer will effectively reduce the electric field near the gate, and the peak value of the electric field near the gate decreases more obviously with the increase of the ε_r value.
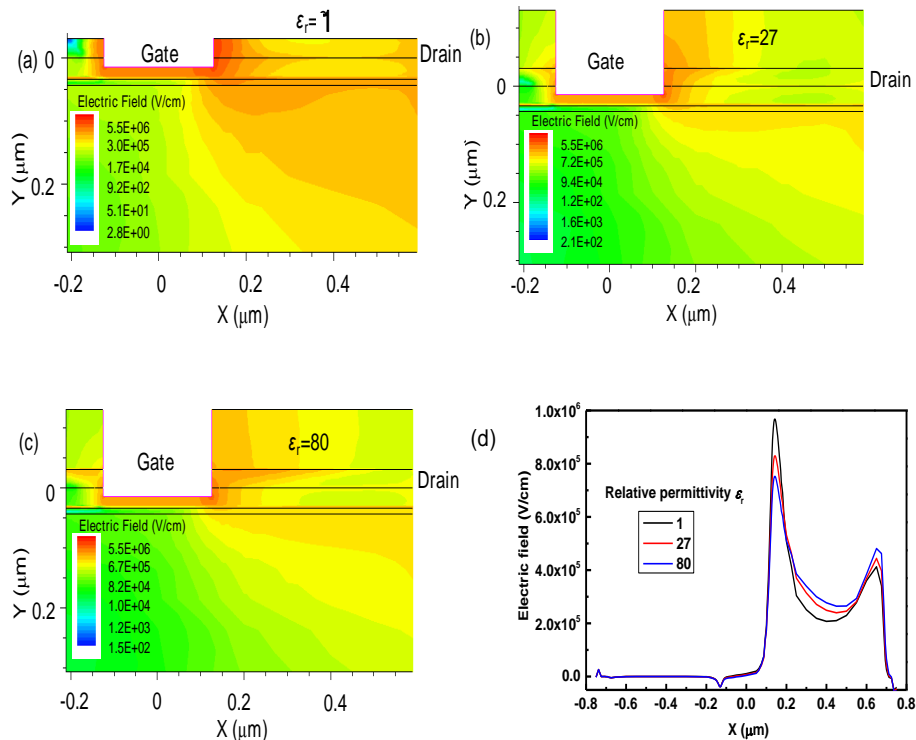
Fig. 5. Electric field distribution at the breakdown voltage with different εr value, (a) 0, (b) 27, (c) 80, (d) Electric field distribution at the interface InGaAs/AlGaAs.

Figure 5 (d) shows the electric field distribution at the InGaAs/AlGaAs heterogeneous. As can be seen from the figure, the peak electric field near the gate decreased by 20% when the ε_r value was 80. In addition, the electric field near the drain increased with the higher ε_r value, leading to an increase in the electron-hole ionization probability at the bottom of the grid-drain

area. Under the action of the electric field, the ionized holes will enter the channel and neutralize more electrons, which results in the depletion region expanding to the buffer layer and forming a high-resistance area, thus bears a higher reverse voltage. Figure 6 shows the variation of the impact ionization rate at the breakdown of the device with different ε_r values. The results showed that with the increase of ε_r, the ionization rate near the gate decreased, while that near the drain increased. Therefore, a passivation layer with a high ε_r value can effectively improve the breakdown voltage of the device.
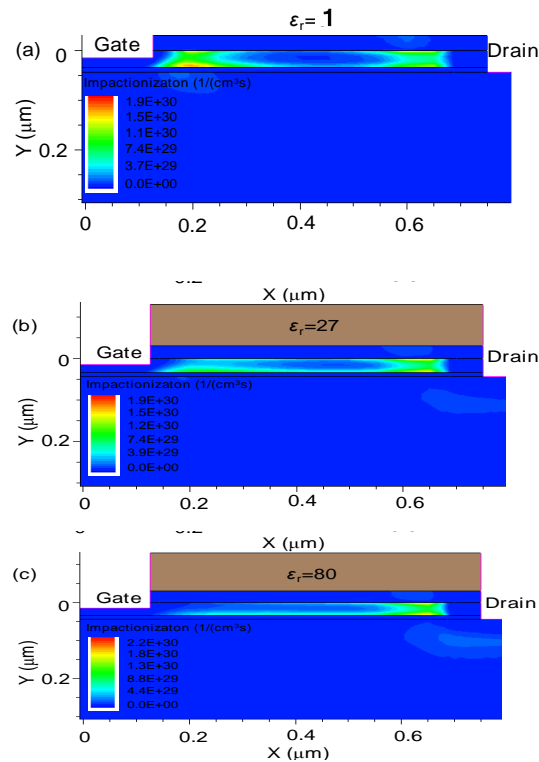
Fig. 6. Impact ionization rates of the device with different ε_r value.

Figure 7 (a) and (b) show the output and transfer characteristics of AlGaAs/InGaAs HEMT with(ε_r=80) and without a passivation layer, respectively. The simulation results showed that I_{DS} and gm decreased slightly after the passivation layer introduced, mainly due to the decreased electron concentration in the channel near the drain.In addition, the conduction resistance values of the two structural devices calculated from Figure 7 (a) were almost unchanged. Therefore, the passivation layer with high ε_r value can effectively improve the breakdown voltage of the device and balance the DC characteristics of the device.
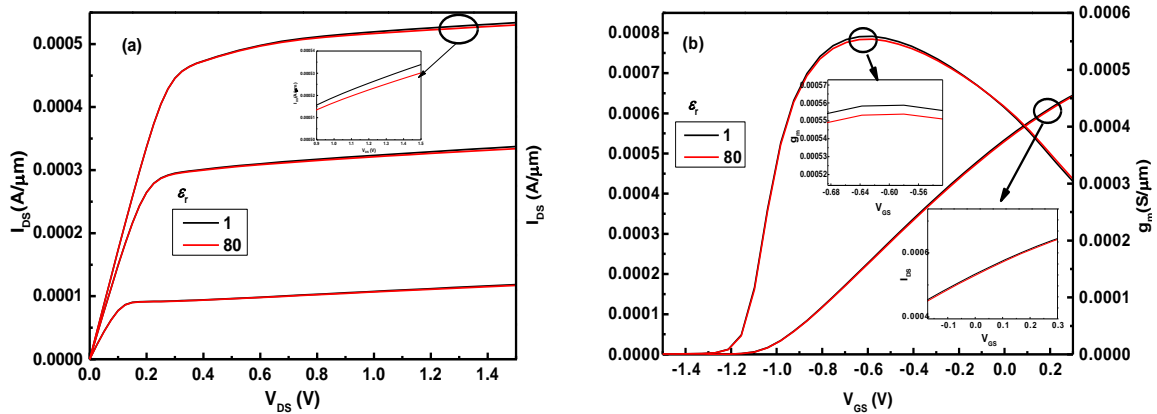
Fig. 7. The output and transfer characteristics of InGaAs/AlGaAs HEMT with and without passivation layer, (a) output characteristics, (b) transfer characteristics.

4. Conclusions

The effect of different passivation layer on the breakdown characteristics of InGaAs/AlGaAs HEMT was analyzed, meanwhile, the influence of the passivation layer on the output and transfer characteristics of the device was also studied. The results showed that the breakdown voltage increased with the ε_r increasing. When the passivation layer with high ε_r value was introduced, the peak value of the electric field near the gate decreased, while the peak value of the electric field near the drain increased, which resulted in the increase of the breakdown voltage of the device. The simulation results of the output and transfer characteristics of the device showed that the passivation layer with high ε_r reduced the I_{DS} and g_m of the device slightly, because the ionization rate near the drain increased with the increase of the ε_r value, leading to the hole capturing electrons in the channel, which reduced the I_{DS} and g_m of the device.In addition, the results show that the introduction of a passivation layer with a high ε_r value causes almost no degradation of the on-resistance.

Acknowledgements

References

[1] J. A. Del Alamo, Nature **479,** 317 (2011).

[2] J. Ajayan, D. Nirmal, Int. J. Electron. **104**, 504 (2016).

[3] C. Zhao, B. Xu, J. Z. Wang, Z. G. Wang, J. Semicond. **41,** 011103 (2020).

[4] J. Ajayan, D. Nirmal, P. Mohankumar, D. Kuriyan, A. S. Augustine Fletcher, L. Arivazhagan, B. Santhosh Kumar, Microelectron. J. **92,** 104604 (2019).

[5] N. Dahbi, R. B. Taleb, O. Zaoui, Journal of Ovonic Research **15,** 167 (2019).

[6] H. C. Gao, Z. J. Yin, Chin. Phys. Lett. **32,** 068102 (2015)

[7] S. J. Cho, C. Wang, N. Y. Kim, Microelectron. Eng. **113,** 11 (2014).

[8] J. Ajayan, D. Nirmal, J. Comput. Electron. **15,** 1291 (2016)

[9] W. Mao, W. B. She, C. Yang, J. F. Zhang, X. F. Zheng, C. Wang, Y. Hao, Chin. Phys. B **25,** 017303 (2016).

[10] Kumari V Neha, M. Gupta, M. Saxena, Adv. Nat. Sci.: Nanosci. Nanotechnol. **10,** 045006 (2019).

[11] T. Kabemura, S. Ueda, Y. Kawada, H. Horio, IEEE T. Electron. Dev. **65,** 3848 (2018).

[12] A. Ajay Soni, M. Shrivastava, IEEE T. Electron. Dev. **67,** 1718 (2020).

[13] C. Joishi, Y. Zhang, Z. Xia, W. Sun, A. R. Arehart, S. Ringel, S. Lodha, S. Rajan, IEEE Electron Device Lett. **40,** 1241 (2019).

[14] H. Hanawa, H. Onodera, A. Nakajima, K. Horio, IEEE T. Electron. Dev. **61,** 769 (2014).

[15] S. Chander, S. Gupta, Gupta M. Ajay, Superlattice. Microst. **120,** 217 (2018).

[16] Y. H. Zhong, J. Yang, X. J. Li, P. Ding, Z. Jin, J. Korean Phys.l Soc. **66,** 1020 (2015).

[17] Y. S. Lin, B. Y. Chen, Microelectron. Eng. **214,** 100 (2019).

[18] B. K. Jebalin, A. S. Rekh, P. Prajoon, N. M. Kumar, D. Nirmal, Microelectron. J. **46,** 1387 (2015).

[19] C. J. Tang, J. X. Shi, Semicond. Sci. Technol. **29,** 125004 (2014)

[20] J. Ajayan, D. Nirmal, P. Mohankumar, L. Arivazhagan, M. Saravanan, S. Saravanan, J. Nanoelectron. Optoe. **14,** 1133 (2019).

[21] S. X. Sun, L. H. Ma, C. Cheng, C. Zhang, Y. H. Zhong, Y. X. Li, P. Ding, Z. Jin, Phys. Status Solidi A **214,** 1700322 (2017).

[22] M. Khalid, J. K. Khan, A. D. Chandio, Z. A. Gilani, Asghar H M N Ul H. Khan, S. Riaz, S. Naseem, Journal of Ovonic Research **14,** 459 (2018).

[23] T. Kabemura, S. Ueda, Y. Kawada, K. Horio, IEEE T. Electron. Dev. **65,** 3848 (2018).

[24] Y. Kawada, H. Hanawa, K. Horio, Jan. J. Appl. Phys. **56,** 108003 (2017).

[25] F. Osaka, T. Mikawa, T. Kaneda, IEEE J. Quantum Elect. **21,** 1334 (1985).

[26] H. Hanawa, K. Horio, Phys. Status Solidi A **211,** 784 (2014).